

# Synthesis and Characterization of Poly(butylene terephthalate) Nanocomposite Fibers: Thermo-Mechanical Properties and Morphology

Jin-Hae Chang, Mu Kyung Mun

Department of Polymer Science and Engineering, Kumoh National Institute of Technology, Kumi 730-701, Korea

Received 1 April 2005; accepted 29 July 2005

DOI 10.1002/app.23500

Published online in Wiley InterScience (www.interscience.wiley.com).

**ABSTRACT:** Nanocomposites of poly(butylene terephthalate) (PBT) with the organoclay C<sub>12</sub>PPH-MMT were prepared using *in situ* intercalation polymerization. Hybrids with various organoclay contents were processed for fiber spinning to examine their thermal behavior, tensile mechanical properties, and morphologies for various draw ratios (DRs). The thermal properties ( $T_g$ ,  $T_m$ , and  $T_D$ ) of the hybrid fibers were found to be better than those of pure PBT fibers and were unchanged by variation of the organoclay loading up to 2 wt %. However, these thermal properties remained unchanged

for DRs ranging from 1 to 18. Most clay layers were dispersed homogeneously in the matrix polymer, although some clusters were also detected. The tensile properties of the hybrid fibers increased gradually with increasing C<sub>12</sub>PPH-MMT content at DR = 1. However, the ultimate strengths and initial moduli of the hybrid fibers decreased markedly with increasing DR. © 2006 Wiley Periodicals, Inc. *J Appl Polym Sci* 100: 1247–1254, 2006

**Key words:** fibers; nanocomposites; organoclay; polyesters

## INTRODUCTION

Poly(butylene terephthalate) (PBT) is used worldwide as an engineering plastic and has many useful properties, including good thermal stability, excellent flow properties, and good chemical resistance.<sup>1–3</sup> However, PBT has poor mechanical properties and a low heat distortion temperature. Many attempts have been made to improve these properties of PBT by blending it with various fillers.<sup>4–6</sup> Among these blends, polymer nanocomposites with organo-modified clays are the materials most commonly used for this purpose. With the addition of only a few percent of clay, polymer nanocomposites exhibit mechanical, thermal, and barrier properties that are greatly improved over those of the pristine polymers. Numerous methods for the preparation of polymer nanocomposites have recently been developed by several groups.<sup>7–10</sup>

Many papers have reported the preparation of polyester nanocomposites, using *in situ* intercalation polymerization. This technique enables the preparation of polymer nanocomposites with a satisfactory degree of exfoliation, which cannot be achieved by direct mixing of polymer and clay. *In situ* intercalation polymeriza-

tion is also particularly attractive because of its versatility and compatibility with the use of reactive monomers, and is beginning to be used in commercial applications.<sup>11–15</sup>

The synthesis of polyester nanocomposites has not been as successful as for other polymer nanocomposites. Some researchers have prepared polyester nanocomposites with quaternary ammonium salt modified clay using the *in situ* intercalation polymerization method,<sup>16,17</sup> but did not find good clay dispersion in the nanocomposites or improved mechanical properties. A more commercial method that uses conventional polymer processing approaches is melt intercalation of the polyester with the organoclay.<sup>18</sup> However, this approach has been far less successful, because it usually leads to poorly dispersed clay particles. This may be due to the low decomposition temperature of the organic modifier bound to the clay surface.<sup>19</sup> To obtain nanocomposites without thermal degradation during processing at temperatures of 250°C and above, an organoclay that is thermally stable at temperatures higher than the process temperatures must be used.<sup>20–24</sup>

This study describes the thermomechanical properties of hybrid fibers that combine PBT as the matrix polymer with a thermally stable organoclay. To improve the tensile properties of the fibers, we tried to optimize processing parameters such as the draw ratio and the organoclay content. The morphological properties of the hybrid fibers were studied using electron microscopy.

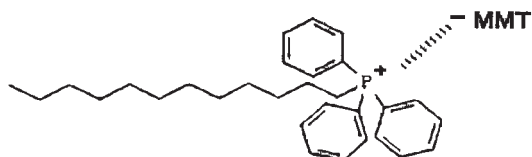
Correspondence to: J.-H. Chang (changjinhae@hanmail.net).

Contract grant sponsor: Korea Science and Engineering Foundation; contract grant number: R05-2003-000-10438-0.

## EXPERIMENTAL

### Materials

All reagents were purchased from Aldrich Chemical (Seoul, Korea), TCI (Tokyo, Japan), and Junsei Chemical. The organically modified montmorillonite, denoted C<sub>12</sub>PPh-MMT, that we used in this study was obtained through a multistep procedure.<sup>24</sup> The chemical structure of C<sub>12</sub>PPh-MMT is as follows:



### Preparation of the C<sub>12</sub>PPh-MMT/PBT nanocomposites

All of the samples were prepared as melts. Since the synthesis procedures for all the hybrids were very similar, only a representative example, the procedure for the preparation of the nanocomposite containing 2 wt % organoclay is described here. 1,4-Butane diol (BD, 90.1 g) (1.0 mol) and 2.24 g of C<sub>12</sub>PPh-MMT were placed in a polymerization tube; the mixture was stirred for 30 min at room temperature. Dimethyl terephthalate (DMT, 90.1 g) (0.5 mol) and 60 mg ( $2.1 \times 10^{-4}$  mol) of isopropyl titanate were placed in a separate tube, and the organoclay/BD system was added to this mixture. Mechanical stirring was used to obtain a homogeneously dispersed system. This mixture was heated for 1 h at 190°C under a steady stream of N<sub>2</sub> gas. The temperature of the reaction mixture was then raised to 230°C and maintained there for 2 h under a steady stream of N<sub>2</sub> gas. During this period, continuous generation of methanol was observed. Finally, the mixture was heated for 2 h at 260°C at a pressure of 1 Torr. The product was cooled to room temperature and repeatedly washed with water. It was dried under vacuum at 70°C for 1 day to obtain the nanocomposite.

We tried to synthesize PBT hybrids containing more than 2 wt % organoclay using the *in situ* intercalation approach. However, repeated attempts to polymerize the 3 wt % C<sub>12</sub>PPh-MMT/PBT hybrid all failed because of bubbles produced in the polymerization reactor during the transesterification of DMT and BD. The problem of how to produce high molecular weight polymer hybrids with high organoclay contents without the formation of bubbles remains unresolved. The solution of this problem is an objective of our research.

### Extrusion

The composites were pressed at 235°C and 2500 kg/cm<sup>2</sup> for 2–3 min on a hot press. The resulting ~0.5-mm

thick films were dried in a vacuum oven at 70°C for 24 h and then extruded through the die of a capillary rheometer. The hot extrudates were immediately drawn at constant speed on a take-up machine to form fibers with various draw ratios (DRs). The mean residence time in the capillary rheometer was ~3–4 min.

### Characterization

The thermal properties of the fibers were evaluated using a DuPont model 910 differential scanning calorimeter (DSC) and thermogravimetric analysis (TGA) at a heating rate of 20°C/min under N<sub>2</sub> flow. Wide-angle X-ray diffraction (XRD) measurements were performed at room temperature using a Rigaku (D/Max-III B) X-ray diffractometer with Ni-filtered Co K $\alpha$  radiation. The scanning rate was 2°/min over a range of  $2\theta = 2$ –30°.

The tensile properties of the fibers were determined using an Instron Mechanical Tester (Model 5564) at a crosshead speed of 20 mm/min at room temperature. The experimental uncertainties in the tensile strengths and the moduli were  $\pm 1$  MPa and  $\pm 0.05$  GPa, respectively. The reported properties were obtained as averages of at least 10 individual determinations.

The samples for use in the transmission electron microscope (TEM) measurements were prepared by placing the PBT hybrid fibers into epoxy capsules and then curing the epoxy at 70°C for 24 h in vacuum. The cured epoxies containing the PBT hybrids were then microtomed into 90-nm thick slices, and a layer of carbon, about 3 nm thick, was deposited on each slice on a mesh 200 copper net. TEM photographs of ultrathin sections of the polymer/organoclay hybrid samples were obtained with an EM 912 OMEGA TEM operating at an acceleration voltage of 120 kV.

## RESULTS AND DISCUSSION

### Dispersibility of the organoclay in PBT

The X-ray scattering intensities for the organoclay and the PBT-clay nanocomposite fibers with various clay contents are shown in Figure 1. The measured  $d_{001}$ -spacing of Na<sup>+</sup>-MMT is 11.99 Å ( $2\theta = 8.60^\circ$ ). After cation exchange between Na<sup>+</sup>-MMT and dodecyltriphenylphosphonium chloride (C<sub>12</sub>PPh-Cl<sup>-</sup>), the  $d_{001}$ -spacing was found to be 36.08 Å ( $2\theta = 2.86^\circ$ ). It appears that Na<sup>+</sup> is replaced by C<sub>12</sub>PPh-Cl<sup>-</sup> during the organic modification and that the C<sub>12</sub>PPh-MMT prepared in this study is well dispersed in water. In general, a larger interlayer spacing should assist the intercalation of the polymer chains. It should also lead to easier dissociation of the clay, which results in hybrids with better clay dispersion.<sup>25,26</sup> In addition to the main diffraction peak, an additional sharp peak

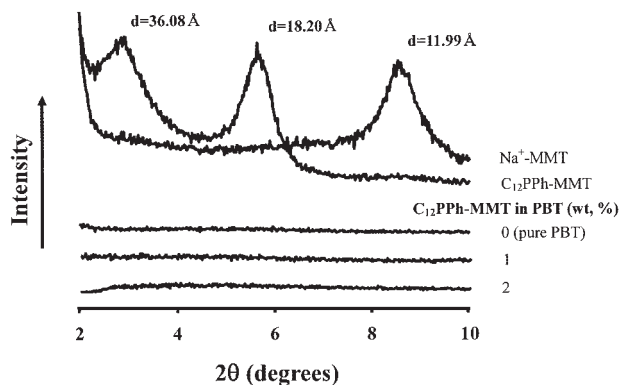


**Figure 1** XRD patterns for clay, organoclay, and PBT hybrid fibers with various organoclay contents.

was observed near  $2\theta = 5.56^\circ$  ( $d = 18.20 \text{ \AA}$ ). This secondary peak is likely to be due to the organoclay.

When the PBT/ $C_{12}$ PPh-MMT hybrid fibers form, the organoclay peak at  $2\theta = 2.86^\circ$  ( $d = 36.08 \text{ \AA}$ ) disappears from the diffraction pattern. This result indicates that the clay layers are exfoliated and dispersed homogeneously in the PBT matrix, and provides supplementary evidence that the PBT/ $C_{12}$ PPh-MMT hybrid fibers are nanocomposites. XRD offers a convenient way to determine the interlayer spacing due to the periodic arrangement of silicate layers in the virgin clay and in intercalated polymer layered hybrids. Although XRD is very useful for measuring the  $d$ -spacing of ordered immiscible and ordered intercalated polymer nanocomposites, it may be insufficient for the analysis of disordered and exfoliated materials with no peaks. The electron microscopy analyses provide the principal evidence in our study for the formation of nanocomposites.

Figure 2 shows the XRD results for the PBT nanocomposites containing 2 wt %  $C_{12}$ PPh-MMT with various DRs. No clay peak was found when DR = 1, nor when DR was increased from 1 to 18. We suggest that higher stretching of the fiber during extrusion leads to better dispersion of the clay, and that this results in a more highly exfoliated morphology.

### Morphology

SEM and TEM were used to visually evaluate the degree of intercalation and the amount of aggregation of clay clusters. It is instructive to consider the size and distribution of the clay particles as a prelude to understanding the morphology of the polymer nanocomposites seen in the micrographs. The morphologies of the extruded fibers obtained from hybrid systems containing up to 2 wt %  $C_{12}$ PPh-MMT in a PBT matrix were examined by observing their fracture surfaces with a SEM, and the results are shown in Figures 3 and 4. Figure 3 shows clay phases that were formed

in undrawn hybrid fibers with organoclay content ranging from 0 to 2 wt %. The PBT hybrid fibers with 0–2 wt %  $C_{12}$ PPh-MMT have morphologies consisting of clay domains, 80–100 nm in size, well dispersed in a continuous PBT phase. Figure 4 shows micrographs of 2 wt %  $C_{12}$ PPh-MMT/PBT hybrid fibers obtained at DRs ranging from 1 to 18. The 2 wt % hybrid fiber with DR = 12 contains fine clay phases 60–110 nm in diameter [see Fig. 4(b)]. The hybrid fiber with DR = 18 also exhibits fine dispersion with domains 30–50 nm in diameter [see Fig. 4(c)]. The domain size of the dispersed clay phase was found to decrease with increasing DR. The fine dispersion of the clay seems to be the result of the stretching of the fiber that occurs when the extrudates pass through the capillary rheometer.<sup>27–30</sup>

More direct evidence of the formation of true nanocomposites is provided by TEM micrographs of the ultramicrotomed sections. The TEM micrographs in Figures 5 (1 wt %) and 6 (2 wt %) attempt to show the structures of the fibers by using different magnifications. Fewer aggregates are visible in Figure 5 than those in Figure 6, since the clay content in the 1 wt % sample is lower. Increasing the magnification in an area occupied by an aggregate reveals that the individual sheets of clay are clearly separated by a layer of polymer, as shown in Figures 5(b) and 6(b). Thus, the morphology consists of a mix of intercalated and exfoliated sheets, that is, there are regions where a regular stacking arrangement is maintained with a layer of polymer between the sheets, and also regions where completely delaminated sheets are dispersed individually.

This TEM micrograph shows that most of the organoclay layers were exfoliated and dispersed homogeneously in the PBT matrix, although some clusters/agglomerates were also detected. This is inconsistent with the XRD results shown in Figure 1. Similar results have been reported by Galgali et al.<sup>31</sup> and Vaia et al.<sup>18</sup> They observed no characteristic clay patterns in their XRD results, even for partially exfoliated nano-

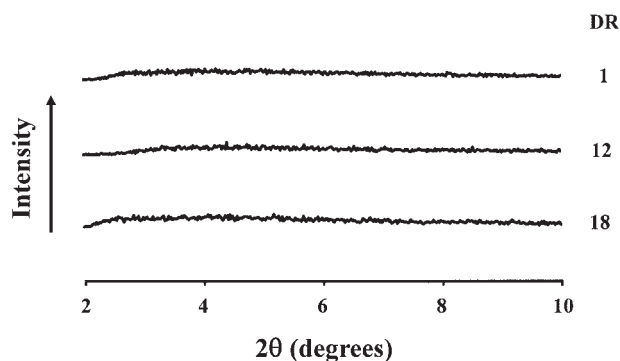


**Figure 2** XRD patterns of 2 wt %  $C_{12}$ PPh-MMT in PBT hybrid fibers with different DRs.

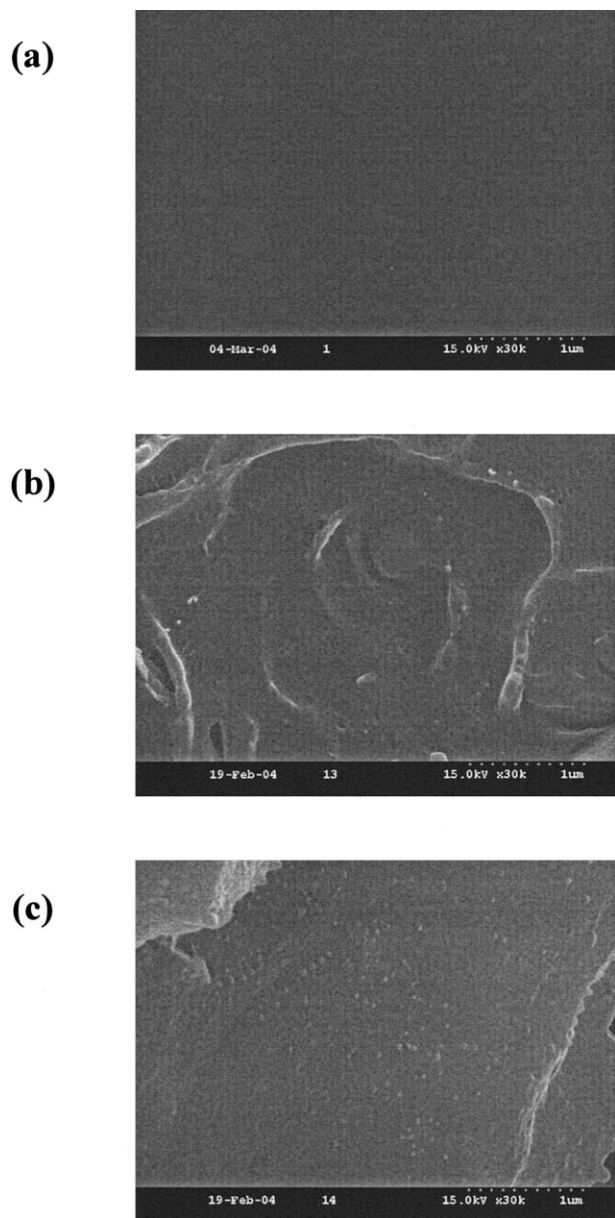


**Figure 3** SEM micrographs of (a) 0 wt % (pure PBT), (b) 1 wt %, and (c) 2 wt %  $C_{12}$ PPh-MMT in PBT hybrid fibers.

structures. They explained this apparent contradiction by noting that TEM provides a qualitative understanding of nanostructures through direct visualization, whereas XRD offers a convenient way to determine the interlayer spacing due to the periodic arrangement of silicate layers in virgin clay and in intercalated polymer/clay hybrids. However, in the exfoliated state where periodic arrangement is lost, XRD does not provide definitive information regarding the structure of nanocomposites.

In conclusion, we were able to successfully synthesize PBT nanocomposites using  $C_{12}$ PPh-MMT via an *in situ* intercalation method. Taking into account these results, we now discuss how the state of the clay

particles affects the thermal behavior and tensile mechanical properties of the organoclay/polymer hybrids.

### Thermal properties

The thermal properties of the PBT hybrids with various organoclay contents are listed in Table I. The polymer hybrids are soluble in the mixed solvent phenol/1,1,2,2-tetrachloroethane, which was used in the measurement of solution viscosity. The inherent solu-

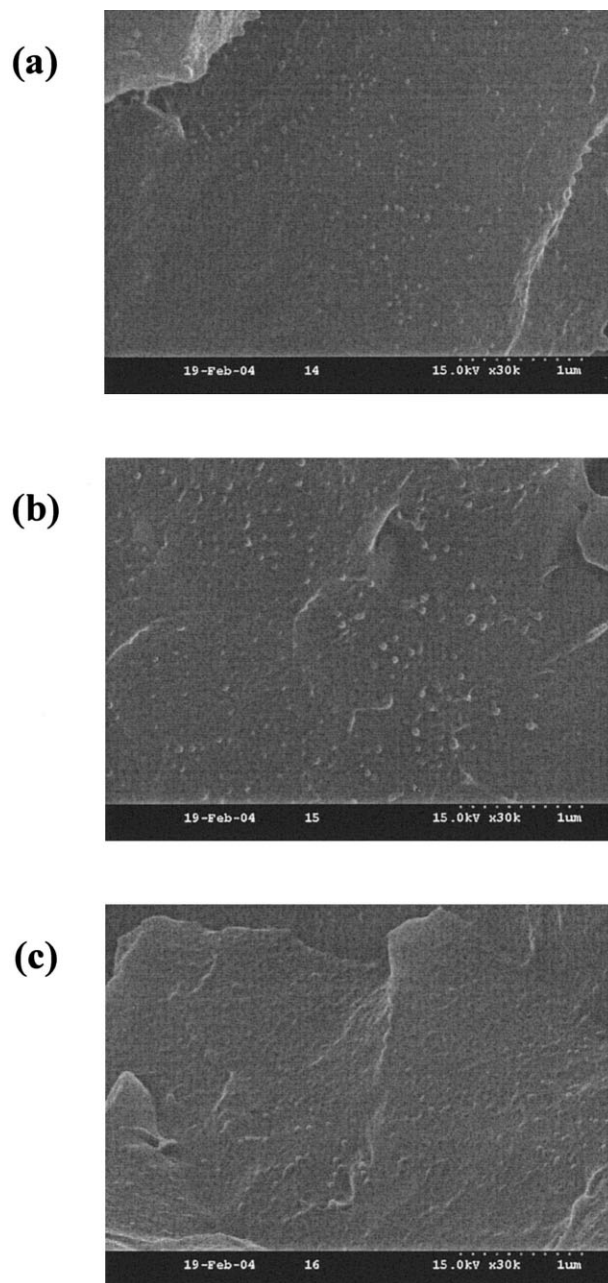


**Figure 4** SEM micrographs of 2 wt %  $C_{12}$ PPh-MMT in PBT hybrid fibers for DRs = (a) 1, (b) 12, and (c) 18.

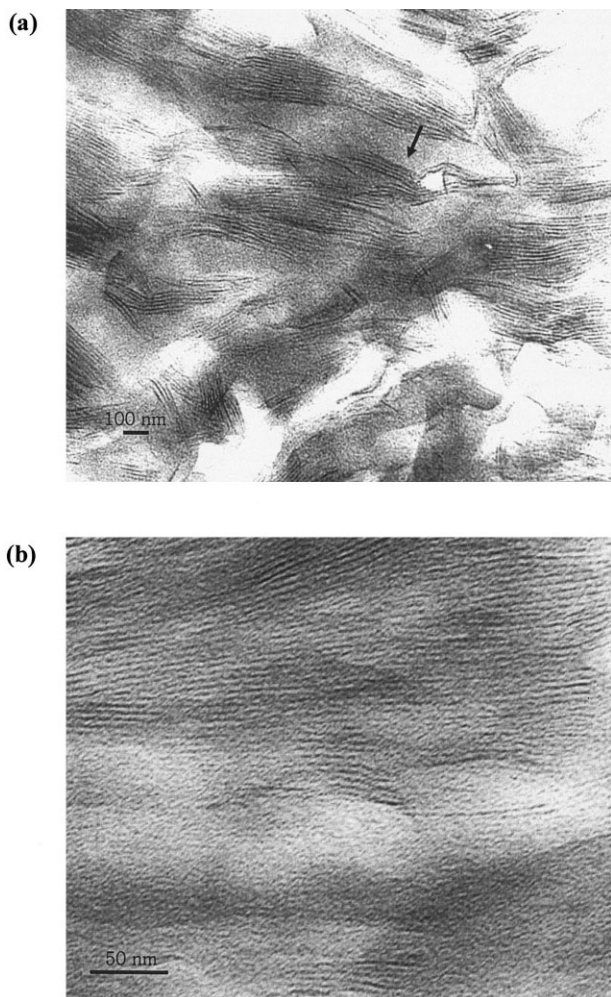


**Figure 5** TEM micrographs of 1 wt %  $C_{12}PPh$ -MMT in PBT hybrid fibers increasing the magnification levels from (a) to (b).

tion viscosity numbers (see Table I) range from 0.80 to 0.95.

The glass transition temperatures ( $T_g$ ), melting temperatures ( $T_m$ ), and initial decomposition temperatures ( $T_D^i$ ) of the hybrids increase with increasing  $C_{12}PPh$ -MMT content up to 1 wt % and then remain constant with further increases in the organoclay loading. For example, the  $T_g$ ,  $T_m$ , and  $T_D^i$  of PBT hybrid fibers with 1 wt % clay loading are higher by 9, 5, and 6°C, respectively, than those of pure PBT, and are not significantly different for 2 wt % clay content. It seems that the thermal properties of the samples are independent of the amount of organoclay in the PBT matrix, as shown in Table I. The observed increase in the glass transition temperatures of these hybrids with the addition of the organoclay could be the result of several different factors, in particular, the increase in crosslink density and the restriction of the segmental relaxation of the chain segments near the clay layers. Similar results have also been obtained in other stud-

ies of polymer nanocomposites.<sup>32,33</sup> The increase in  $T_m$  with the addition of organoclay may result from the enhanced heat insulation effect of the clay layer structure, as well as from the enhanced interaction between the organoclay and the PBT molecular chains.<sup>34,35</sup> The addition of clay also enhances the initial decomposition temperatures by acting as a superior insulator and as a mass-transport barrier to the volatile products generated during decomposition.<sup>36–38</sup> The TGA curves for the clay, the organoclay, and the PBT hybrid fibers with various organoclay contents are shown in Figure 7.

In contrast to the thermal properties, the weight of the residue at 600°C increased monotonically with increases in the clay loading from 0 to 2%, ranging from 1 to 10% as shown in Table I. This enhancement of the char formation with increasing organoclay content is ascribed to the high heat resistance of the clay.

Considering the aforementioned results, we conclude that the introduction of inorganic components into organic polymers can improve their thermal sta-

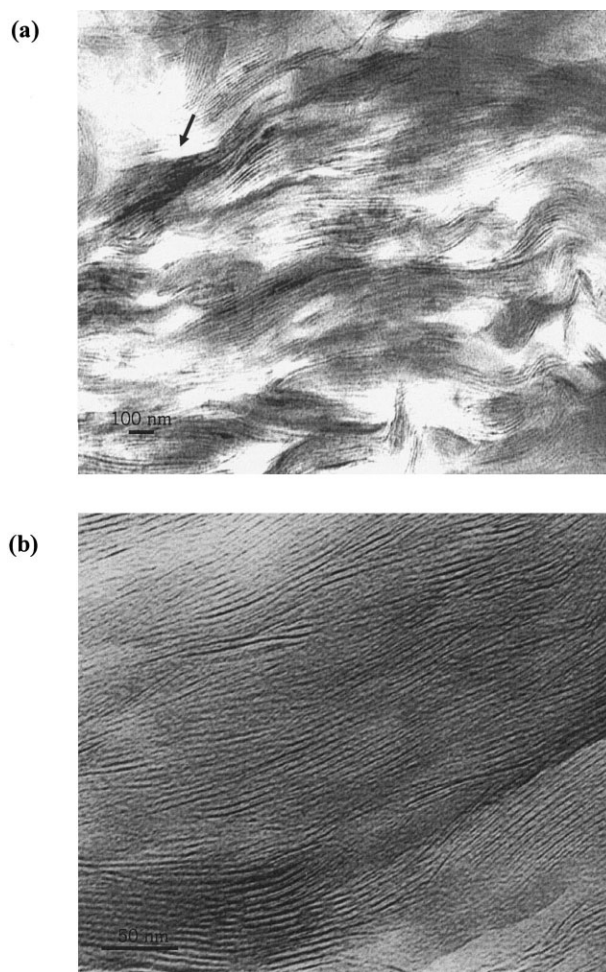


**Figure 6** TEM micrographs of 2 wt %  $C_{12}PPh$ -MMT in PBT hybrid fibers increasing the magnification levels from (a) to (b).

**TABLE I**  
Thermal Properties of PBT Hybrid Fibers

Organoclay (wt %)	DR <sup>a</sup>	IV <sup>b</sup>	T <sub>g</sub> (°C)	T <sub>m</sub> (°C)	ΔH <sup>c</sup> (J/g)	T <sub>D</sub> <sup>id</sup> (°C)	wt <sub>R</sub> <sup>600e</sup> %
0 (pure PBT)	1	0.85	27	222	40	371	1
1	1	0.95	36	227	41	377	6
2	1	0.80	37	227	41	375	10
2	12		36	227	41	376	10
2	18		36	227	41	376	10

<sup>a</sup> Draw ratio.

<sup>b</sup> Inherent viscosities were measured at 30°C by using 0.1 g/100 mL solutions in a phenol/1,1,2,2-tetrachloroethane (w/w = 50/50) mixture.

<sup>c</sup> Enthalpy changes of melting transition temperature.

<sup>d</sup> Initial weight-loss onset temperature.

<sup>e</sup> Weight percent of residue at 600°C.

bilities. For this hybrid system, the largest improvement in the thermal properties was found for a loading of C<sub>12</sub>PPH-MMT of only 1 wt %. For the PBT hybrid fibers containing 2 wt % organoclay, the thermal properties were constant for variation of DR in the range from 1 to 18.

### Mechanical properties

The mechanical tensile properties of the PBT hybrid fibers for various C<sub>12</sub>PPH-MMT contents and various DRs are shown in Table II. It can be seen that the ultimate strengths of the hybrids increase gradually with increasing organoclay content and are highest for a clay content of 2 wt % and DR = 1. The ultimate tensile strengths of the hybrids were found to increase from 41 to 58 MPa with an increase in the organoclay content to 2 wt %. This improvement was possible because organoclay layers could be dispersed and intercalated in the PBT matrix. This result is consistent with the general observation that the introduction of an organoclay into a matrix polymer increases its tensile strength.<sup>39–41</sup> A similar trend was observed for the initial modulus. The modulus values were found to increase linearly with increasing organoclay content.

When the C<sub>12</sub>PPH-MMT content was increased to 2 wt %, the modulus of the hybrid was found to be 3.33 GPa, about 2.5 times as great as that of pure PBT (1.37 GPa). This increased initial modulus could be the result of two different factors: the high resistance exerted by the clay, and the orientation and the aspect ratio of the clay layers. Further, increasing the clay content increases the constraints on the polymer chain mobility, which also increases the modulus.<sup>42,43</sup>

Thus, low loadings of C<sub>12</sub>PPH-MMT were found to be sufficient to improve the mechanical properties of the PBT hybrid fibers. This is attributed to the strong interaction between PBT and the organoclay that arises from the formation of nanocomposites with fine dispersion.

The increases in the tensile strength and the initial modulus with DR were insignificant for pure PBT. For pure PBT, the strength and the modulus increased from 41 to 46 MPa and 1.37 to 1.71 GPa, respectively, as the DR was increased from 1 to 18, as shown in Table II. Unlike flexible coil-like polymers,<sup>44–46</sup> the values of the ultimate strength and the initial modulus of the hybrid fibers decreased markedly with increasing DR, as shown in Table II. For hybrid fibers with 1

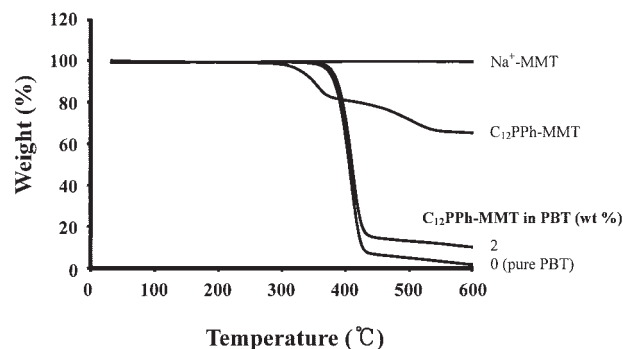


**Figure 7** TGA thermograms of clay, organoclay, and PBT hybrid fibers with different organoclay contents.

**TABLE II**  
Tensile Properties of PBT Hybrid Fibers

Organoclay (wt %)	DR <sup>a</sup>	Ult. Str. (MPa)	Ini. Mod. (GPa)	EB <sup>b</sup> (%)
0 (pure PBT)	1	41	1.37	3
	12	43	1.69	3
	18	46	1.71	3
1	1	55	2.96	3
	12	52	2.57	3
	18	48	2.33	2
2	1	58	3.33	2
	12	35	2.45	2
	18	28	2.21	2

<sup>a</sup> Draw ratio.

<sup>b</sup> Elongation percent at break.

wt %  $C_{12}$ PPh-MMT, as DR was increased from 1 to 18, the tensile strength and the initial modulus decreased from 55 to 48 MPa and from 2.96 to 2.33 GPa, respectively. Similar trends were observed for the hybrid fiber with 2 wt %  $C_{12}$ PPh-MMT. This decline in the ultimate strength and the initial modulus seems to be the result of debonding between the organoclay and the matrix polymer and the presence of many nano-sized voids because of excess stretching of the fibers. It has clearly been shown<sup>47,48</sup> that an imperfect inclusion/matrix interface cannot sustain the large interfacial shear stress that develops as a result of an applied strain. The percent elongations at break of all the samples were 2–3%. These values were found to be independent of the organoclay loading and DR. The variations in the ultimate strengths and the initial moduli of the PBT hybrid fibers are plotted against clay content for varying DR in Figures 8 and 9, respectively.

### CONCLUSIONS

PBT nanocomposites were fabricated from monomers and organoclay via an *in situ* intercalation polymerization method. PBT nanocomposites with various organoclay contents were melt-spun at various DRs to produce monofilaments. Most of the  $C_{12}$ PPh-MMT organoclay we used was found to be exfoliated and dispersed homogeneously in the PBT polymer, providing direct evidence that the  $C_{12}$ PPh-MMT/PBT hybrid fibers formed nanocomposites. This conclusion was confirmed using XRD and TEM. In general, the thermal properties ( $T_{g'}$ ,  $T_{m'}$  and  $T_D^i$ ) of the hybrid fibers were observed to increase as the clay content was increased from 0 to 1 wt % and did not change further with the addition of further organoclay, i.e., at

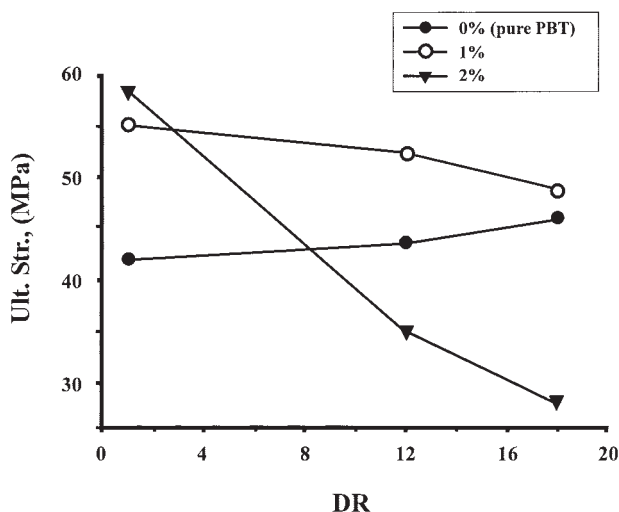


**Figure 8** Effects of DR on the ultimate tensile strength of organoclay contents.

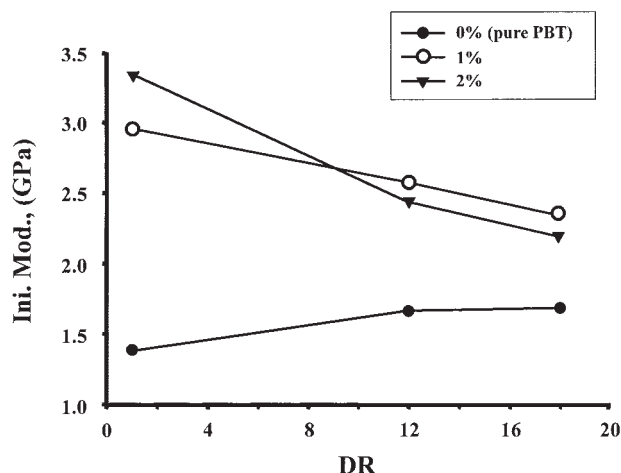


**Figure 9** Effects of DR on the initial tensile modulus of organoclay contents.

2 wt % loading. Hybrids with various organoclay contents were extruded at various DRs from a capillary rheometer to investigate their mechanical properties. The ultimate strengths and initial moduli of the hybrid fibers were found to increase with increasing organoclay content at DR = 1. When the amount of organoclay in PBT reached 2 wt %, a 1.5-fold increase in the ultimate strength and a 2.5-fold increase in the initial modulus were obtained, with respect to pure PBT. In this system, it was found that small additions of organoclay were enough to improve the properties of the matrix polymer, PBT. However, the ultimate strengths and the initial moduli of the PBT hybrid fibers decreased significantly with increasing DR because of debonding around the polymer–clay interfaces and void formation.

### References

- Runt, J.; Miley, D. M.; Zhang, X.; Gallagher, K. P.; McFeaters, K.; Fishburn, J. *Macromolecules* 1992, 25, 1929.
- Sasaki, A.; White, J. L. *J Appl Polym Sci* 2003, 90, 1839.
- Jeon, H. K.; Kim, J. K. *Polymer* 1998, 39, 6227.
- Li, X.; Kang, T.; Cho, W. J.; Lee, J. K.; Ha, C. S. *Macromol Rapid Commun* 2001, 22, 1306.
- Chang, J. H.; Farris, R. J. *Polym J* 1995, 27, 780.
- Chang, J. H.; Jo, B. W. *J Appl Polym Sci* 1996, 60, 939.
- Okada, A.; Usuki, A. *Mater Sci Eng* 1995, C3, 109.
- Gilman, J. W. *Appl Clay Sci* 1999, 15, 31.
- Giannelis, E. P. *Adv Mater* 1996, 8, 29.
- Wang, Z.; Lan, T.; Pinnavaia, T. *J Chem Mater* 1996, 8, 2200.
- Blumstein, A. *J Polym Sci Polym Chem* 1995, 31, 119.
- Fukushima, Y.; Okada, A.; Kawasumi, M.; Kurauchi, T.; Kamigaito, O. *Clay Miner* 1988, 23, 27.
- Akelah, A.; Moet, A. *J Mater Sci* 1996, 31, 3589.
- Messersmith, P. B.; Giannelis, E. P. *Chem Mater* 1993, 5, 1064.
- Hwang, S. H.; Paeng, S. W.; Kim, J. Y.; Huh, W. *Polym Bull* 2003, 49, 329.
- Takekoshi, T.; Khouri, F. F.; Campbell, J. R.; Jordan, T. C.; Dai, K. H. U.S. Pat. 5,530,052, (1996).

17. Li, X.; Park, H. M.; Lee, J. O.; Ha, C. S. *Polym Eng Sci* 2002, 42, 2156.
18. Vaia, R. A.; Jandt, K. D.; Kramer, E. J.; Giannelis, E. P. *Chem Mater* 1996, 8, 2628.
19. Matayabas, J. C., Jr.; Turner, S. R. In *Polymer Clay Nanocomposites*; Pinnavaia, T. J., Ed.; Wiley: New York, 2000.
20. Zhu, J.; Morgan, A. B.; Lamelas, F. J.; Wilkie, C. A. *Chem Mater* 2001, 13, 3774.
21. Zhu, J.; Uhl, F. M.; Morgan, A. B.; Wilkie, C. A. *Chem Mater* 2001, 13, 4649.
22. Saujanya, C.; Imai, Y.; Tateyama, H. *Polym Bull* 2002, 49, 69.
23. Davis, C. H.; Mathias, L. J.; Gilman, J. W.; Schiraldi, D. A.; Shields, J. R.; Trulove, P.; Sutto, T. E.; Delong, H. C. *J Polym Sci Part B: Polym Phys* 2002, 40, 2661.
24. Chang, J.-H.; Kim, S. J.; Im, S. *Polymer* 2004, 45, 5171.
25. Hsiao, S. H.; Liou, G. S.; Chang, L. M. *J Appl Polym Sci* 2001, 80, 2067.
26. Ke, Y.; Lu, J.; Yi, X.; Zhao, J.; Qi, Z. *J Appl Polym Sci* 2000, 78, 808.
27. Kohli, A.; Chung, N.; Weiss, R. A. *Polym Eng Sci* 1989, 29, 573.
28. Dutta, D.; Fruitwala, H.; Kohli, A.; Weiss, R. A. *Polym Eng Sci* 1990, 30, 1005.
29. Blizard, K. G.; Baird, D. G. *Polym Eng Sci* 1987, 27, 653.
30. Weiss, R. A.; Huh, W.; Nicolais, L. *Polym Eng Sci* 1987, 27, 684.
31. Galgali, G.; Ramesh, C.; Lele, A. *Macromolecules* 2001, 34, 852.
32. Li, F.; Ge, J.; Honigfort, P.; Fang, S.; Chen, J. C.; Harris, F.; Cheng, S. *Polymer* 1999, 40, 4987.
33. Agag, A.; Takeichi, T. *Polymer* 2000, 41, 7083.
34. LeBaron, P. C.; Wang, Z.; Pinnavaia, T. *J Appl Clay Sci* 1999, 12, 11.
35. Hussain, M.; Varley, R. J.; Mathys, Z.; Cheng, Y. B.; Simon, G. P. *J Appl Polym Sci* 2004, 91, 1233.
36. Fomes, T. D.; Yoon, P. J.; Hunter, D. L.; Keskkula, H.; Paul, D. R. *Polymer* 2002, 43, 5915.
37. Fischer, H. R.; Gielgens, L. H.; Koster, T. P. M. *Acta Polym* 1999, 50, 122.
38. Petrovic, X. S.; Javni, L.; Waddong, A.; Banhegyi, G. J. *J Appl Polym Sci* 2000, 76, 133.
39. Lan, T.; Pinnavaia, T. *J Chem Mater* 1994, 6, 2216.
40. Masenelli-Varlot, K.; Reynaud, E.; Vigier, G.; Varlet, J. *J Polym Sci Part B: Polym Phys* 2002, 40, 272.
41. Yano, K.; Usuki, A.; Okada, A. *J Polym Sci Part A: Polym Chem* 1997, 35, 2289.
42. Chen, L.; Wong, S. C.; Pisharath, S. *J Appl Polym Sci* 2003, 88, 3298.
43. Kojima, Y.; Usuki, A.; Kawasumi, M.; Okada, A.; Fukushima, Y.; Kurauchi, T.; Kamigaito, O. *J Mater Res* 1993, 8, 1185.
44. La Mantia, F. P.; Valenza, A.; Paci, M.; Magagnini, P. L. *J Appl Polym Sci* 1989, 38, 583.
45. Chen, T. K.; Tien, Y. I.; Wei, K. H. *Polymer* 2000, 41, 1345.
46. Liu, X.; Wu, Q. *Polymer* 2001, 42, 10013.
47. Curtin, W. A. *J Am Ceram Soc* 1991, 74, 2837.
48. Shia, D.; Hui, Y.; Burnside, S. D.; Giannelis, E. P. *Polym Eng Sci* 1987, 27, 887.